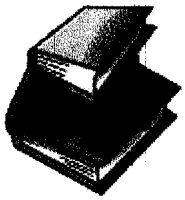
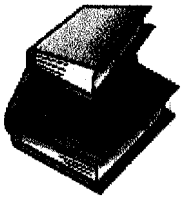
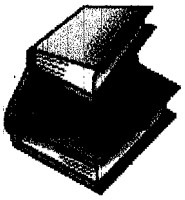

Carnegie Mellon University
Engineering & Science Library
Interlibrary Loan
(412) 268-7215

Ariel IP 128.2.24.31

Date:_____

Please return this cover sheet, along with a copy of the original request if there are any transmittal problems:

- ☐ Missing Pages
- ☐ Edges Cut off
- ☐ Unable to Read
- ☐ Other

Pages Needed:

ILL Number:

OCLC Symbol:

ILLiad TN: 55651

Lending String: *PMC,LYU,PVU,UCW,GSU

Patron: Henson, Michael

Journal Title: Journal of process control.

Volume: 12 **Issue:** 6
Month/Year: 2002
Pages: 721-734

Article Author:

Article Title: Zhang YC, Zamamiri AM, Henson MA, and Hjortso MA; Cell population models for bifurcation analysis and nonlinear control of continuous yeast
biore

Imprint: Guildford, Surrey, UK ; Butterworth-Hein

ILL Number: 9561194

Call #:

Location: BND-JOUR

Item #:

ARIEL

Borrower: AUM Invoice 14 pgs.

Shipping Address:
W.E.B. Du Bois Library- ILL
University of Massachusetts
Box 34710, 154 Hicks Way
Amherst, MA 01003
Fax:
Ariel: 128.119.169.34

ELSEVIER

Journal of Process Control 12 (2002) 721–734

JOURNAL OF PROCESS CONTROL

www.elsevier.com/locate/jprocont

Cell population models for bifurcation analysis and nonlinear control of continuous yeast bioreactors

Yongchun Zhang, Abdelqader M. Zamamiri, Michael A. Henson*, Martin A. Hjortsø

Department of Chemical Engineering, Louisiana State University, Baton Rouge, LA 70803-7303, USA

Received 12 December 2000; received in revised form 27 March 2001; accepted 27 March 2001

Abstract

Saccharomyces cerevisiae (baker's yeast) can exhibit sustained oscillations over a wide range of operating conditions when produced in a continuous bioreactor. In this paper the bifurcations leading to these periodic solutions are investigated using an unstructured, segregated model in which the population balance equation (PBE) for the cell mass distribution is coupled to the mass balance of the rate limiting substrate. The PBE model is shown to produce periodic solutions over a range of dilution rates due to the presence of two supercritical Hopf bifurcations. The problem of oscillation attenuation using nonlinear feedback control with four candidate input/output variable pairings is investigated. The controller designs are based on a low dimensional moment representation of the PBE model. The performance of the nonlinear controllers are compared and discussed. © 2002 Elsevier Science Ltd. All rights reserved.

Keywords: Biochemical reactor; Distributed parameter system; Bifurcation analysis; Feedback linearization

1. Introduction

Saccharomyces cerevisiae (baker's yeast) is an important micro-organism in the brewing, baking, food manufacturing and genetic engineering industries. Many investigators have shown that continuous cultures of *Saccharomyces cerevisiae* exhibit sustained oscillations in glucose limited environments under aerobic growth conditions [2,19,21–23,28,30]. A precise characterization of the environmental conditions that support oscillatory dynamics has not been developed because oscillations often appear and disappear without any measurable change in external inputs such as nutrient flow and concentration. The underlying cellular mechanisms that cause oscillatory yeast dynamics are controversial and have been a subject of three decades of intensive research. Understanding and controlling this dynamic behavior would lead to important advances in yeast production processes and could provide key insights into the cellular behavior of more complex eucaryotic cells present in plants and animals.

A number of transient models have been proposed to explain the sustained oscillations observed in continuous cultures of baker's yeast. Existing models can be classified into three categories: structured and unsegregated [3,8,14]; unstructured and segregated [1,6,10,12]; and structured and segregated [4,26,27]. Structured models account for various chemical components and their interactions within the cell. By contrast unstructured models are based on the simplifying assumption that detailed modeling of intracellular behavior is not essential to describe cell growth. Segregated models account for differences between individual cells in terms of properties such as cell mass or cell age. Unsegregated models are based on the simplifying assumption that individual cells have identical physical and chemical properties.

Oscillatory dynamics produced by structured, unsegregated models are a direct result of cell metabolism incorporated into the model. For example in the cybernetic model proposed in [14] oscillations arise from competition between three metabolic pathways: glucose fermentation, glucose oxidation and ethanol oxidation. A shortcoming of purely metabolic models is that they cannot adequately explain cell cycle synchronization that leads to the formation of distinct cell subpopula-

* Corresponding author. Tel.: +1-225-388-1476; fax: +1-225-338-1476.

E-mail address: henson@che.lsu.edu (M.A. Henson).

PII: S0959-1524(01)00010-5

tions. It is well known that synchronization plays a critical role in the stabilization of oscillatory yeast dynamics [21,23,24].

In unstructured, segregated models oscillations arise due to cell population dynamics rather than individual cell metabolism. The key feature of these models is a population balance equation (PBE) that describes the time evolution of the cell age or cell mass distribution. Sustained oscillations can be generated by coupling the PBE and the extracellular environment to establish a synchrony induction mechanism [9]. While they are capable of predicting cell cycle synchrony, these models cannot capture the interplay between cell metabolism and oscillatory dynamics due to their unstructured nature [14]. Structured, segregated models have been developed to address the limitations of the simpler models described above. The most sophisticated model of this type is presented in [27]. A discretized form of the cell mass distribution is combined with a metabolic model that accounts for basic intracellular variables such as storage carbohydrates. The model is capable of producing sustained oscillations with periods comparable to those observed experimentally. However the model is not well suited for control applications due to its complexity.

Our previous work [33] has shown that an unstructured, segregated model in which the PBE for the cell mass distribution is coupled to the mass balance of the rate limiting substrate can predict sustained oscillations. However, the underlying mechanism that leads to periodic solutions has not been investigated. Since the appearance and disappearance of periodic solutions are attributable to bifurcation phenomenon, a detailed bifurcation analysis will provide key insights into the PBE model structure and may motivate further experimental studies aimed at verifying the model predictions. Such a bifurcation study is presented in this paper.

We have used the PBE model to develop a linear model predictive control (LMPC) strategy for attenuating and inducing sustained oscillations in continuous yeast bioreactors [33]. The linear controller design model is obtained by linearizing and temporally discretizing the nonlinear ordinary differential equations derived from spatial discretization of the PBE model. The resulting linear state-space model is used to develop LMPC controllers that regulate the discretized cell number distribution by manipulating the dilution rate and feed substrate concentration. While our simulation tests have been encouraging, the LMPC strategy suffers from several potential disadvantages including: (i) the controller design model is linear even though bifurcations are a nonlinear phenomenon; (ii) the cell mass distribution is assumed to be measured or reconstructed from particle size measurements; (iii) the resulting control problem is highly non-square (2 inputs, 14 outputs); and (iv) direct control of the cell distribution is complex and often unnecessary as typical end products are metabolites rather than the yeast population itself. In this paper we develop nonlinear controllers that are easier to implement and provide improved performance.

The remainder of this paper is organized as follows. Our relevant experimental and modeling work is described in Section 2. The application of bifurcation analysis techniques to the cell population model is discussed in Section 3. Nonlinear controller design based on a moment representation of the PBE model and closed-loop simulation results are presented in Section 4. A summary and conclusions are presented in Section 5.

2. Cell population model for continuous yeast bioreactors

2.1. Experimental data

There is a large body of experimental data on the transient behavior of intracellular and extracellular variables during sustained oscillations of continuous yeast cultures. It is well known that yeast cultures exhibit oscillations only for a specific range of dilution rates [22]. Stationary solutions are observed for dilution rates below and above this range. We have conducted additional experiments in our laboratory to explore these oscillatory dynamics. Batch and continuous culture experiments were performed using a Bioflo 3000 fermenter (New Brunswick) with a working volume of 1.0 l interfaced to a personal computer with the necessary software for data collection and basic regulatory control functions. Details on the medium preparation and experimental protocol are available in [31].

One set of experiments was designed to test our hypothesis that a stable steady-state and a periodic attractor can co-exist at the same operating conditions. A representative set of results for a glucose feed concentration of 30 g/l is shown in Fig. 1. The evolved carbon dioxide signal is used as a representative output variable for the culture. The experiment starts with oscillatory dynamics that are obtained by switching the culture from batch to continuous operation. At $t = 20$ h the dilution rate is slowly ramped down over a 24 h period until the oscillations disappear. The stationary state is preserved for 2 days while the dilution rate is maintained at the low dilution rate value. At $t = 92$ h the dilution rate is slowly ramped up at the same rate as used for the negative ramp. No significant oscillations are observed when the dilution rate is maintained at the high value despite the fact that a slightly lower dilution rate produced oscillations at the beginning of the experiment.

An enlarged view of the dynamic behavior during the first and last parts of the experiment is shown in Fig. 2. The upper plot shows the large amplitude oscillations

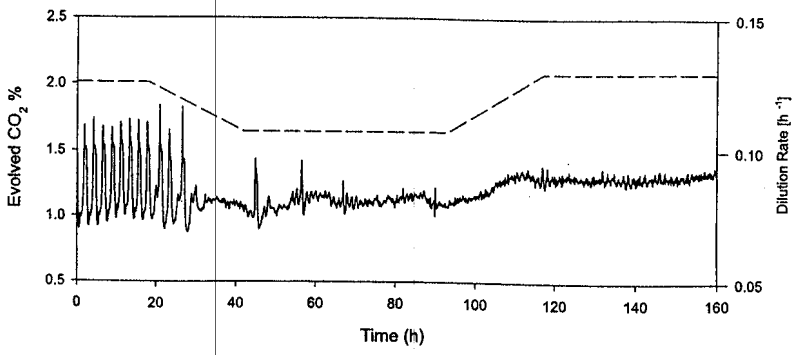

Fig. 1. Experimental ramp changes in dilution rate.

obtained at the beginning of the experiment. The lower plot shows the response observed at the end of the experiment. The evolved CO_2 signal in the lower plot appears to represent a stationary solution. This suggests the co-existence of a stable steady state and a periodic attractor at the same dilution rate. When examined more carefully the signal in the lower plot appears to contain a periodic component that is not solely attributable to measurement noise. It is possible that this steady-state solution actually is unstable but appears to be stable due to the relatively short duration of the test. Consequently the long-term stability of this "stationary" solution is questionable. We currently are conducting experiments aimed at resolving this issue. Nevertheless a candidate yeast model should be capable of capturing this apparent hysteresis behavior.

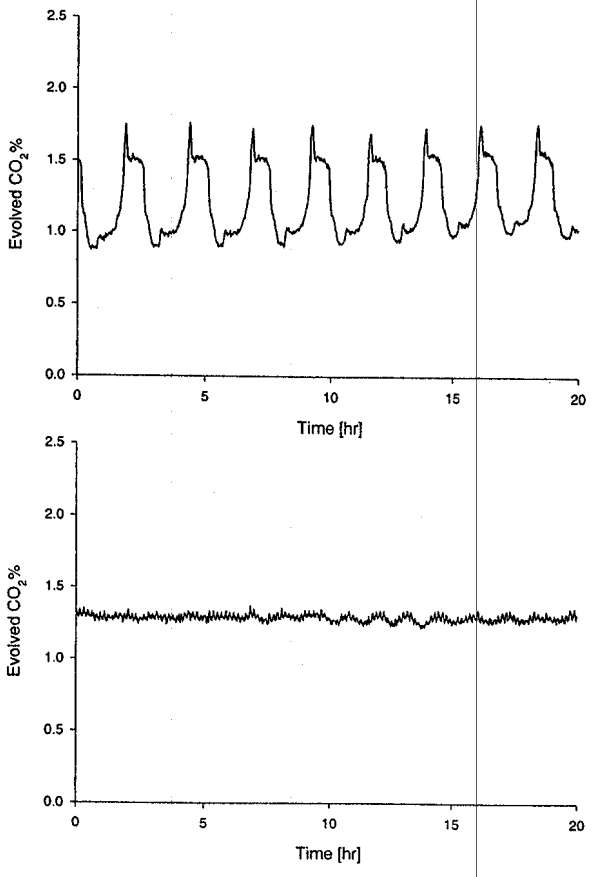

Fig. 2. Experimentally observed solutions under the same operating conditions.

2.2. Cell population model equations

Zhu et al. [33] propose a cell population model for budding yeast cultures which can be used to predict operating conditions under which periodic solutions exist. The model couples the PBE for the cell mass distribution to the substrate mass balance. The simplified cell cycle from which the PBE model is derived is shown in Fig. 3. A daughter cell grows until it reaches a critical mass called the transient mass (m_t^*). At this point the cell is called a mother cell. All further growth occurs in the bud attached to the mother cell. At a critical mass called the division mass (m_d^*) the mother cell and the bud divide to produce a newborn daughter cell and a newborn mother cell. The critical masses that characterize the cell cycle depend on the extracellular conditions as discussed below.

We briefly present the PBE model equations to facilitate the subsequent development. Additional details are available in [33]. The PBE has the form:

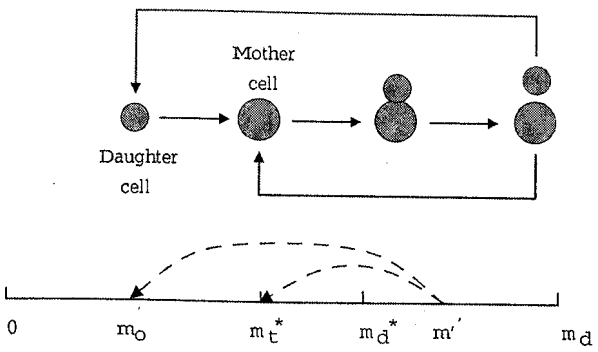

Fig. 3. Simplified cell cycle model for budding yeast.

$$\frac{\partial W(m,t)}{\partial t}+\frac{\partial[k(S')W(m,t)]}{\partial m} = \int_0^{\infty} 2p(m,m')\Gamma(m',S')W(m',t)\mathrm{d}m' - [D+\Gamma(m)]W(m,t) \quad (1)$$

where: m is the cell mass; $W(m,t)$ is the cell number density; $k(S')$ is the single cell growth rate; S' is the filtered substrate concentration (defined below); $p(m,m')$ is the newborn cell probability function; $\Gamma(m,S')$ is the division intensity function; and D is the dilution rate. The initial cell distribution is denoted $W(m,0)$ and the boundary condition is $W(0,t)=0$. The zeroth moment of the cell number density represents the total number of cells per unit volume and is defined as: $m_0(t)=\int_0^{\infty} W(m,t)\mathrm{d}m$. The differential equation describing the evolution of the zeroth moment is easily derived [15]:

$$\frac{\mathrm{d}m_0}{\mathrm{d}t} = -Dm_0 + \int_0^{\infty}\Gamma(m,S')W(m,t)\mathrm{d}m \quad (2)$$

The division intensity function is modeled as:

$$\Gamma(m,S') = \begin{cases} 0 & m \leqslant m_t^* + m_a \\ \gamma\exp\left[-\varepsilon\left(m-m_d^*\right)^2\right] & m\in\left[m_t^*+m_a, m_d^*\right] \\ \gamma & m\geqslant m_d^* \end{cases} \quad (3)$$

where m_t^* is the transition mass, m_a is the additional mass that mother cells must gain before division is possible, ϵ and γ are constant parameters and m_d^* is the division mass at which the division intensity function reaches its maximum value γ. The newborn cell probability function $p(m,m')$ is chosen as:

$$p(m,m') = A\exp\left[\beta\left(m-m_t^*\right)^2\right] + A\exp\left[\beta\left(m-m'+m_t^*\right)^2\right] \quad (4)$$

when $m<m'$ and $m'>m_t^*+m_a$; the function is identically zero otherwise. Here A and β are constant parameters. This function yields two Gaussian peaks in the cell number distribution, one centered at the transition mass m_t^* (which corresponds to mother cells) and one centered at a location in the mass domain that is determined by mass conservation (which corresponds to daughter cells).

As suggested by available experimental data [33], the transition mass m_t^* and the division mass m_d^* are modeled as increasing functions of the substrate concentration:

$$m_t^*(S') = \begin{cases} m_{t0}+K_t(S_l-S_h) & S'<S_l \\ m_{t0}+K_t(S'-S_h) & S'\in[S_l,S_h] \\ m_{t0} & S'>S_h \end{cases} \quad (5)$$

$$m_d^*(S') = \begin{cases} m_{d0}+K_d(S_l-S_h) & S'<S_l \\ m_{d0}+K_d(S'-S_h) & S'\in[S_l,S_h] \\ m_{d0} & S'>S_h \end{cases} \quad (6)$$

where S_l, S_h, m_{t0}, m_{d0}, K_t and K_d are constant parameters. The substrate mass balance is:

$$\frac{\mathrm{d}S}{\mathrm{d}t} = D(S_f-S) - \int_0^{\infty}\frac{k(S')}{Y}W(m,t)\mathrm{d}m = D(S_f-S) - \frac{k(S')}{Y}m_0 \quad (7)$$

where Y is a constant cell mass yield coefficient. The single cell growth rate is assumed to follow Monod kinetics:

$$k(S') = \frac{\mu_m S'}{K_m+S'} \quad (8)$$

where the maximum growth rate μ_m and the saturation parameter K_m are constants. The filtered substrate concentration is generated as:

$$\frac{\mathrm{d}S'}{\mathrm{d}t} = \alpha(S-S') \quad (9)$$

where the constant parameter α indicates how fast cells respond to environmental changes.

The parameters used for model simulation are listed in Table 1. Only a few of the parameter values (e.g. single cell growth rate constants) are available in the literature. Therefore, the unknown parameters are chosen heuristically to yield reasonable bioreactor operating conditions and experimentally observed dynamic behavior. The key parameters for generation of sustained oscillations are the exponent ϵ of the division intensity function (3) and the slope K_d of the division mass function (6). These parameters must be sufficiently large to create the attractive force that leads to the formation of distinct cell subpopulations. The oscillation period is same for all variables and is most strongly affected by the dilution rate (i.e. the reactor residence

Table 1
Cell population model parameters

Variable	Value	Variable	Value
γ	200 h^{-1}	ε	5×10^{22} g^{-2}
A	$\sqrt{25/\pi}\times10^{11}$ g^{-1}	β	100×10^{22} g^{-2}
S_l	0.1 g/l	S_h	2 g/l
K_t	0.01×10^{-11} g/g l	K_d	2×10^{-11} g/g l
m_{to}	6×10^{-11} g	m_{d0}	11×10^{-11} g
m_{max}	12×10^{-11} g	m_a	1×10^{-11} g
Y	0.4 g/g	μ_m	5×10^{-10} g/h
K_m	25 g/l	α	20 h^{-1}
D	0.25 h^{-1}	S_f	25 g/l

time). Because the oscillation amplitude of each variable is different, it is difficult to adjust the model parameters to obtain agreement with experiment. It is important to emphasize that the cell population model can be expected only to yield predictions that are in qualitative agreement with experiment. As part of our future work we intend to investigate the estimation of unknown model parameters from experimental data generated in our laboratory.

2.3. Numerical solution of the cell population model

The PBE model is comprised of a coupled set of nonlinear algebraic, ordinary differential and integro-partial differential equations. Analytical solution is possible only under very restrictive assumptions [11,12]. A variety of numerical solution techniques based on finite difference, weighted residual and orthogonal collocation methods have been developed for such PBE models [17,18,29]. In this paper the solution technique based on orthogonal collocation on finite elements proposed by Zhu et al. [33] is used. The mass domain is discretized into a number of finite elements, each of which contains several collocation points where the PBE is approximated by an ODE. Integral terms are approximated using Gaussian quadrature. The state vector of the resulting nonlinear ODE model consists of the cell number density at each collocation point, as well as the substrate and filtered substrate concentrations. We use 12 finite element and 8 internal collocation points on each finite element to yield a total of 111 state variables.

The dynamic response of the cell population model to a dilution rate ramp test similar to that performed experimentally (see Fig. 1) is shown in Fig. 4. The substrate concentration (S) is used as the output variable since the PBE model does not describe the evolved CO_2 concentration. While not considered in this paper, it is worth noting that we have developed a structured description of the extracelluar environment that allows the PBE model predictions to be compared more directly to extracellular variables measured in our laboratory [20]. The dilution rate is ramped down from the oscillatory region ($D=0.21\ h^{-1}$) to the non-oscillatory region ($D=0.18\ h^{-1}$) and then ramped back up to the original dilution rate. The simulated oscillation period (2.5 h) is very close to the value observed experimentally (2.2 h). However, the simulated negative ramp leads to very slow damping of the oscillations as compared to that observed experimentally. On the other hand, the simulated positive ramp produces oscillations of a much smaller amplitude than those observed during the initial portion of the test. It is difficult to ascertain if the model predictions are consistent with experimental data due to the questions surrounding the stability of the steady-state solution in the oscillatory range. A more thorough analysis of the PBE model behavior is possible using bifurcation analysis.

3. Bifurcation analysis

Bifurcation analysis is a powerful tool for studying the dynamic behavior of nonlinear models. We are interested in characterizing the bifurcations that lead to the appearance and disappearance of periodic solutions in the yeast cell population model. This will allow a more insightful comparison to experimental data than is

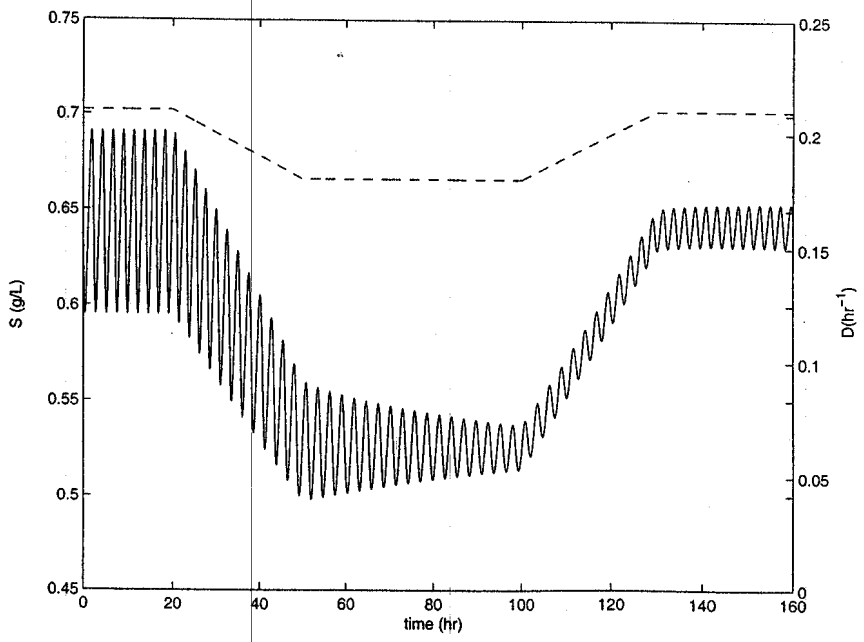

Fig. 4. Simulated ramp changes in dilution rate.

possible with dynamic simulation alone. The vast majority of bifurcation theory is developed for nonlinear ODE systems [16]. Consequently, it is necessary to spatially discretize the PBE model prior to analysis. Given the complexity of the resulting model, numerical bifurcation techniques must be pursued as theoretical analysis is not possible.

3.1. Computational methods

It is well known that yeast cultures exhibit sustained oscillations only for a specific range of dilution rates [22]. This suggests that the dilution rate is an appropriate choice for the bifurcation parameter. As the dilution rate is increased the PBE model should exhibit two bifurcations corresponding to the appearance and disappearance of sustained oscillations.

The first task is to determine the local stability of steady-state solutions for different values of the bifurcation parameter. Steady-state solutions are obtained by solving the steady-state version of the spatially discretized PBE model using the nonlinear algebraic equation solver FSOLVE available in MATLAB. The Jacobian matrix is generated analytically by linearizing the nonlinear model at the steady state solution. Local stability of the steady state is determined by computing the eigenvalues of the Jacobian using the MATLAB routine EIG. A dilution rate where one or more eigenvalues cross the imaginary axis is known as a bifurcation point [16].

Locating periodic solutions and determining their stability is a much more difficult problem. A stable periodic solution can be located by dynamic simulation if the initial condition is in the domain of attraction. In addition to being restricted to stable solutions, this approach is time consuming and subject to misinterpretation if the oscillatory solution exhibits slow divergence from periodicity. A more efficient and reliable alternative is to use the shooting method to locate both stable and unstable periodic solutions [16]. To achieve convergence a good initial guess of the state variables and the oscillation period corresponding to the periodic solution must be supplied. For stable periodic solutions, the initial guess is obtained readily by dynamic simulation.

The shooting method involves the following iterative calculation procedure. First the model is integrated over one oscillation period. The difference between the initial and ending points is used to adjust the values of the state vector and the period. During each of these Newton iterations, one preselected state variable is fixed to provide a basis for determining the period. This is known as the pinning condition. The iterations continue until a convergence criterion is satisfied. The procedure is repeated for other dilution rates using a process known as continuation [16] such that it is necessary to provide an initial guess only at one value of the bifurcation parameter.

The shooting method effectively transforms the n-dimensional continuous-time system into an $(n-1)$-dimensional discrete-time system. The Poincaré map transforms a periodic solution of the continuous-time system to a fixed point on the $(n-1)$-dimensional hyperplane [16]. Stability of the periodic solution is determined by examining the magnitude of the Floquet multipliers which characterize the stability of the linearized Poincaré map. There always is a single Floquet multiplier of unity magnitude due to the translational invariance of the solution in time. The periodic solution is stable if the remaining $n-1$ Floquet multipliers are inside the unit circle.

Several continuation packages have been developed for detailed bifurcation analysis of low-dimensional systems. The high dimensionality of the discretized cell population model ($x \in \Re^{111}$) precludes the use of such general purpose continuation packages. We have obtained from Professor Yannis Kevrekidis (Princeton) a continuation code based on the numerical techniques discussed above that is specifically designed to locate limit cycles of high-dimensional systems. Stability of the periodic solution is determined from the associated Floquet multipliers. The ODE solver ODESSA is used for numerical integration. A limitation of the code is that it only allows one-parameter bifurcation analysis.

3.2. Results

A bifurcation diagram for the spatially discretized cell population model is shown in Fig. 5 where the dilution rate (D) is the bifurcation parameter and the substrate concentration (S) is chosen as a representative output variable. The feed substrate concentration (S_f) is held constant at 25 g/l. The model possesses a single stable steady-state solution (+) at low dilution rates. As the dilution rate is increased a bifurcation occurs at $D=0.205$ h^{-1} where the steady-state solution becomes unstable (o) and a stable periodic solution with oscillations of the magnitude indicated (*) appears. The spectrum of the Jacobian matrix shows that a pair of eigenvalues cross from the left-half plane (LHP) to the right-half plane (RHP) at this point. This is a supercritical Hopf bifurcation [16] characterized by the appearance of small amplitude oscillations. For a large range of dilution rates the stable periodic solution coexists with the unstable steady-state solution. As the dilution rate is increased to $D=0.285$ h^{-1}, the periodic solution disappears and the steady-state solution regains its stability. The RHP eigenvalues cross back into LHP in a second supercritical Hopf bifurcation.

Fig. 6 shows the spectrum of the discretized cell population model at the steady-state solution for the dilution rate $D=0.25$ h^{-1} located in the middle of the

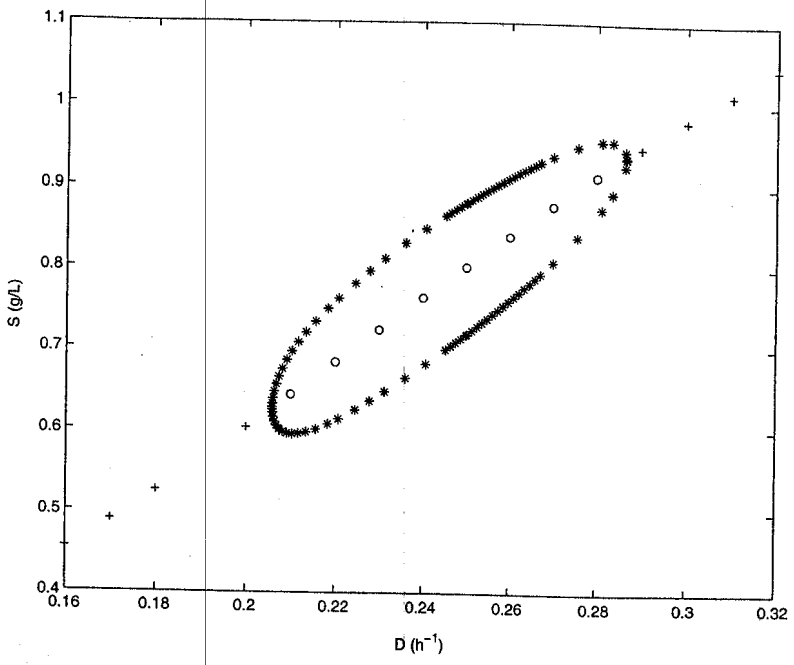

Fig. 5. Bifurcation diagram of the cell population model with dilution rate as the bifurcation parameter.

oscillatory region. The model has a total of 111 eigenvalues due to the number of collocation points used. Many of the eigenvalues (λ_i) are located near the imaginary axis. In particular there is a complex conjugate pair of eigenvalues located in the RHP (see inset). This shows that the steady state is unstable and suggests the existence of a stable periodic solution. Because the RHP eigenvalues are located very close to the imaginary axis, transitions between stable steady-state and stable periodic solutions are quite slow (see Fig. 4). Unless the parameters can be adjusted such that the nature of the bifurcation is changed, this result suggests that the model is incapable of producing the rapid transition observed experimentally for the negative ramp change (see Fig. 1). On the other hand, the supercritical Hopf bifurcation mechanism provides a plausible explanation for the apparent hysteresis behavior observed experimentally for the positive ramp change since the "stationary" solution actually may represent an oscillatory solution of very small amplitude.

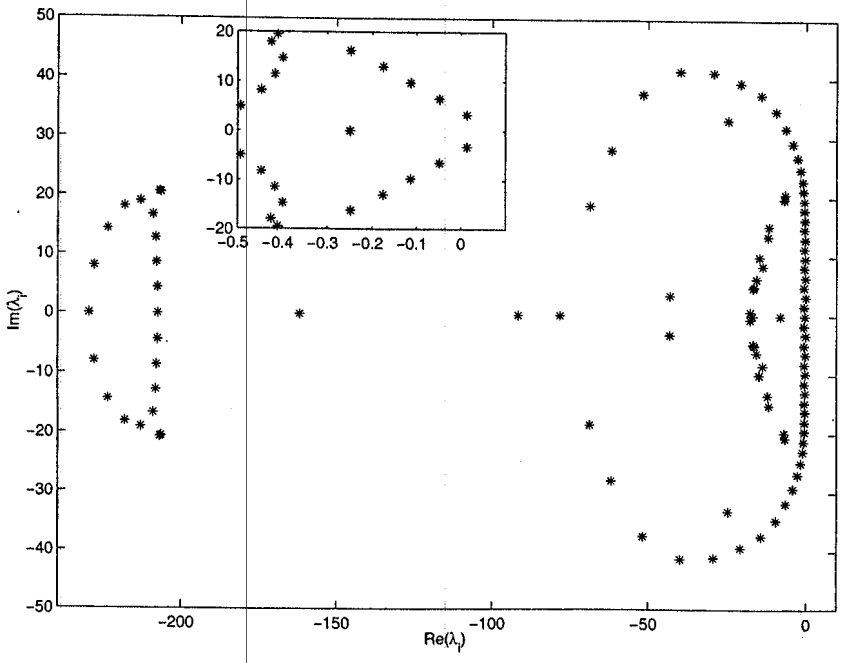

Fig. 6. Spectrum of the cell population model.

Since the feed substrate concentration (S_f) also is a bioreactor input, it is useful to investigate the dynamic behavior of the model with respect to this variable. Fig. 7 shows the bifurcation diagram of the discretized PBE model where S_f is the bifurcation parameter and the substrate concentration S is the output variable. The dilution rate is fixed at 0.25 h^{-1}. For small feed substrate concentration ($S_f < 12.7$ g/l) there is only a single stable steady-state solution. For S_f values above this limit the steady-state solution becomes unstable and a stable period solution is observed. The transition is attributable to a supercritical Hofp bifurcation.

In our previous work we suggested that the steady-state solution is stable at dilution rates that support sustained oscillations [32]. A mechanism involving fold bifurcations of limit cycles [16] was proposed to explain this behaviour. In that work the Jacobian matrices were calculated using finite difference approximation. While all the eigenvalues of the approximate Jacobian matrix are in the left-half plane, a complex conjugate pair of eigenvalues is located very close to the imaginary axis. We have found that the calculation of the approximate Jacobian is numerically ill-conditioned and the associated stability results are not reliable.

In this paper Jacobian matrices are calculated analytically from the discretized PBE model and the bifurcation results have been verified with open-loop simulations using the ODE solver ODESSA. These results indicate that the steady-state solution is unstable at dilution rates that support sustained oscillations. To explore the possible effects of spatial discretization, we have performed the linear stability analysis for $D = 0.25$ h^{-1} and $S_f = 25$ g/l with different numbers of finite elements (n_e) and internal collocation points (n_c). The real part of the complex conjugate pair of eigenvalues ($\lambda_{1,2}$) located closest to the imaginary axis is shown below for different discretizations. The results in Fig. 6 have been generated with $n_e = 12$ and $n_c = 8$.

- $n_e = 12$, $n_c = 8$: $\mathrm{Re}(\lambda_{1,2}) = 0.01382$
- $n_e = 12$, $n_c = 12$: $\mathrm{Re}(\lambda_{1,2}) = 0.01356$
- $n_e = 16$, $n_c = 12$: $\mathrm{Re}(\lambda_{1,2}) = 0.01387$
- $n_e = 24$, $n_c = 16$: $\mathrm{Re}(\lambda_{1,2}) = 0.01362$

The location of the eigenvalues are not affected by different discretizations. Therefore, we are confident that the bifurcation diagrams in Figs. 5 and 7 are indeed correct.

4. Nonlinear control

Control objectives for oscillating yeast cultures can include the attenuation or the stabilization of limit cycles. Clearly the attenuation of undesirable oscillations will lead to improve bioreactor operability under normal conditions. Oscillation stabilization may be desirable in certain situations; e.g. to increase the production of key metabolites produced preferentially during part of the cell cycle. In this work only the oscillation attenuation problem will be investigated. The bifurcation diagrams in Figs. 5 and 7 show that the PBE model has a stable periodic solution and an unstable steady-state solution over a wide range of operating conditions. Our goal is to modify the bifurcation structure such that periodic solutions are rendered unstable under feedback and the desired steady-state solution become globally asymptotically stable.

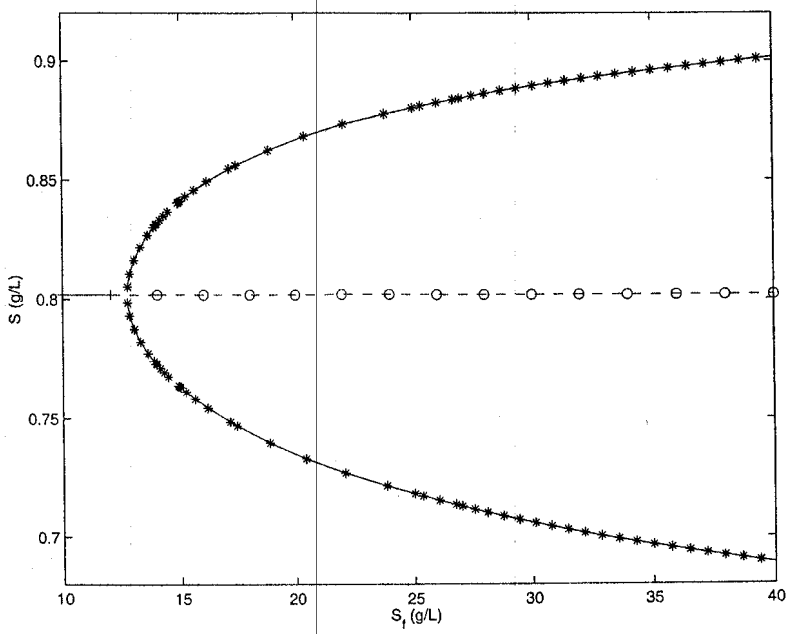

Fig. 7. Bifurcation diagram of the cell population model with feed substrate concentration as the bifurcation parameter.

Ideally this would be achieved through the application of bifurcation-theoretic control techniques [5]. Unfortunately the complexity of the spatially discretized PBE makes this approach intractable. Zhu et al. [33] have developed a linear model predictive control strategy for oscillation attenuation of yeast cultures. As discussed in Section 1 this approach has several potential disadvantages, most notably the use of a linear model for the controller design. Input–output linearization [13] appears to be a good strategy for this problem since it allows the use of a nonlinear model, yet the controller is simple to design and implement. Kurtz et al. [15] have successfully used this approach for the attenuation and stabilization of oscillations in binary fission cultures.

4.1. Controller design issues

The cell population model contains two variables that may serve as manipulated inputs: the dilution rate (D) and the feed substrate concentration (S_f). It is not possible to achieve an arbitrary cell number distribution with these two inputs [33]. As a simple alternative, we consider the cell number concentration (m_0) and the substrate concentration (S) as candidate controlled outputs. Therefore, the finite dimensional model used for nonlinear controller design is:

$$\begin{aligned}\dot{m}_0 &= -Dm_0 + \int_0^\infty \Gamma(m, S')W(m, t)\mathrm{d}m \\ \dot{S} &= D(S_f - S) - \frac{k(S')}{Y}m_0 \\ \dot{S}' &= \alpha(S - S')\end{aligned} \tag{10}$$

First single-input, single-output (SISO) controllers will be designed and evaluated. Then a multiple-input, multiple-output (MIMO) controller will be designed, and the performance of the SISO and MIMO controllers will be compared.

Given the two manipulated inputs (D, S_f) available and the two controlled outputs (m_0, S) chosen, there are a total of four candidate input/output pairings for nonlinear controller design. The D/m_0, D/S and S_f/S pairs have relative degree one [13] since the input affects the output through a single integrator. By contrast, the ODE for m_0 does not include S_f as an input. This input/output pair has a relative degree of three since S_f affects m_0 through the filtered substrate concentration (S') and the substrate concentration (S) equations. Construction of the associated input-output linearizing controller reintroduces the PBE equation through the term $\frac{\partial W}{\partial t}$ that appears in the first time derivative of the m_0 equation. Since the goal of introducing the zeroth moment is to obtain a finite dimensional representation of the cell population model, the S_f/m_0 pair is not used for controller design. Consequently, the input/output pairs considered are D/m_0, D/S and S_f/S.

Using equipment available in our laboratory, m_0 and S can be measured every 10–15 min. Because these measurements are not available continuously, it is necessary to implement discretized approximations of the continuous-time nonlinear controllers. The 10–15 min sampling period is not sufficient for satisfactory performance of the sampled nonlinear controllers. However, state-of-the-art measurement technologies [25] are available that allow the 3 min sampling time assumed in this study.

4.2. Results and discussion

First the D/m_0 pair is considered for nonlinear controller design. The input/output linearizing control law is synthesized directly from the zeroth moment equation:

$$D = \frac{v - \int_0^\infty \Gamma(m, S')W(m, t)\mathrm{d}m}{-m_0} \tag{11}$$

The integral term in this equation represents the growth rate of the cell number concentration due to cell division and can be inferred from common on-line measurements [7]. This integral is assumed to be known in this study. The input v of the feedback linearized system is chosen to place the closed-loop poles and to include integral action for offset error tracking of the setpoint m_0^*:

$$v = -\alpha_1 m_0 + \alpha_0 \int_0^t (m_0^* - m_0)\mathrm{d}\tau \tag{12}$$

where the tuning parameters α_0 and α_1 are chosen such that $s^2 + \alpha_1 s + \alpha_0$ is a Hurwitz polynomial. The second term in the right hand side of (12) is chosen as $-\alpha_1 m_0$ instead of $\alpha_1(m_0^* - m_0)$ to eliminate overshoot in the closed-loop response. It is easy to show that this control law yields the following closed-loop transfer function:

$$g_d(s) = \frac{m_0(s)}{m_0^*(s)} = \frac{\alpha_0}{s^2 + \alpha_1 s + \alpha_0} \tag{13}$$

The desired closed-loop response is obtained by appropriate choice of the controller tuning parameters (α_0, α_1).

The performance of the D/m_0 feedback linearizing controller with $\alpha_1 = 1\ \mathrm{h}^{-1}$ and $\alpha_0 = 0.25\ \mathrm{h}^{-2}$ is shown in Fig. 8. These tuning parameters yield a critically damped second-order response with a time constant of 2 h. The open-loop response (– –) is the stable periodic solution obtained for $D = 0.25\ \mathrm{h}^{-1}$ and $S_f = 25$ g/l. The controller is turned on at $t = 4$ h yielding the closed-loop response shown (—). The ideal response corresponding to the closed-loop transfer function (13) also is shown (· · ·). The setpoint $m_0^* = 1.55 \times 10^{11}$ cells/l is the

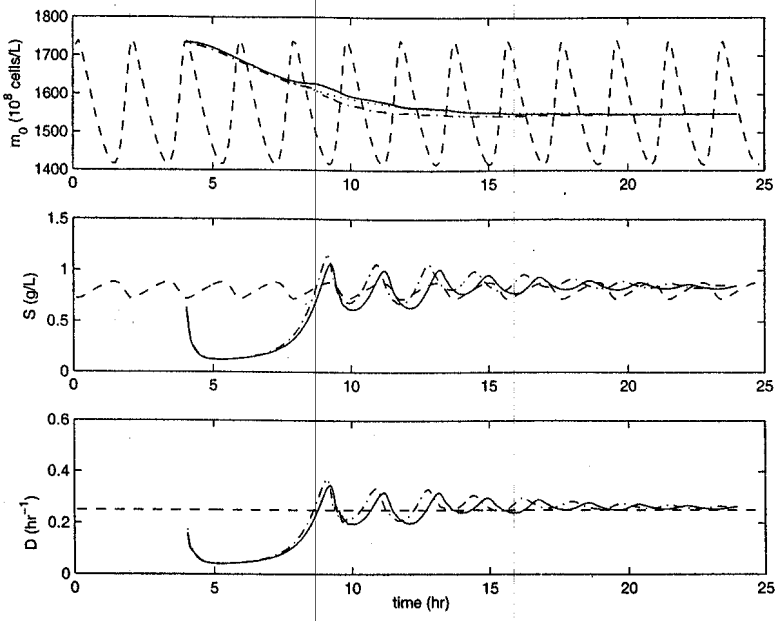

Fig. 8. Feedback linearizing control using the D/m_0 pairing.

total cell concentration for the nominal operating conditions in Table 1. The corresponding steady-state value of the substrate concentration (S) is 0.8 g/l. The controlled output m_0 closely follows the reference trajectory and the oscillations are completely eliminated. Deviations from the ideal closed-loop response are due to sampling. In addition, oscillations in the uncontrolled output S are effectively damped and this variable is driven to its steady-state value. Also shown in Fig. 8 is the closed-loop response (– · –) for a +10% error in the integral that appears in the D/m_0 controller (11). The performance only is slightly degraded as compared to the perfect model case. This test shows that the nonlinear controller has some degree of robustness to such measurements errors.

The cell mass distribution obtained with the D/m_0 controller in the absence of modeling error is shown in Fig. 9. The initial distribution corresponds to a particular point of the stable periodic solution for $D = 0.25$ h^{-1} and $S_f = 25$ g/l. Note the presence of two distinct cell subpopulations that are typical of a synchronized yeast culture [21]. Under open-loop conditions this initial distribution leads to sustained oscillations as seen in Fig. 8. The feedback linearizing controller rapidly

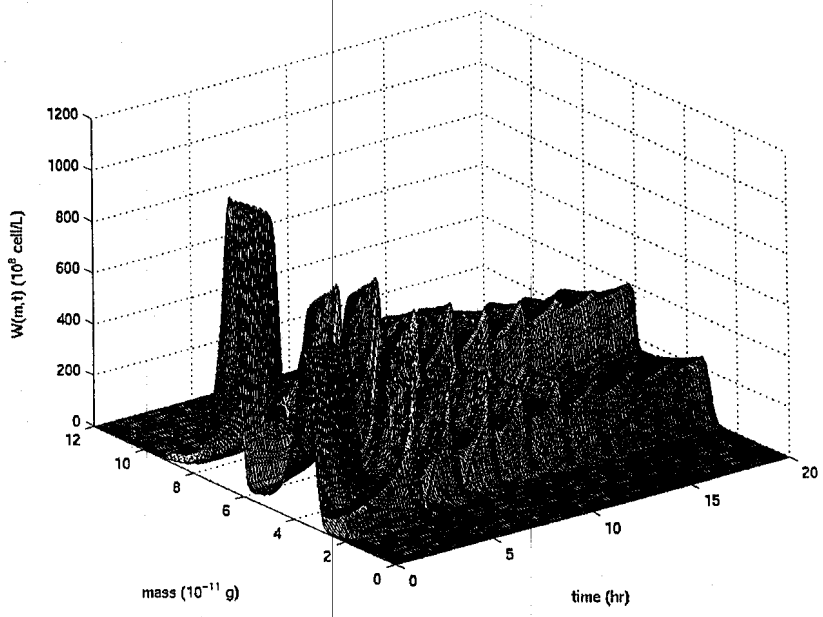

Fig. 9. Cell distribution corresponding to Fig. 8.

drives the culture to a steady-state operating point with a more dispersed cell distribution. This result demonstrates that a nonlinear controller based on the finite-dimensional moment model can yield effective damping of oscillations in the entire cell distribution.

The second controller is designed using the D/S pair. The input/output linearizing control law is synthesized directly from the substrate concentration equation:

$$D = \frac{v + \frac{k(S')}{Y} m_0}{S_f - S} \tag{14}$$

where the input v is:

$$v = -\alpha_1 S + \alpha_0 \int_0^t (S^* - S) d\tau \tag{15}$$

The third controller is designed using the S_f/S pair. The input/output linearizing control law is:

$$S_f = \frac{v + \frac{k(S')}{Y} m_0}{D} + S \tag{16}$$

The input v is chosen as in (15). As compared to the D/m_0 controller (11), an advantage of using S as the controlled output is that the resulting controllers (14) and (16) only require measurements of m_0 and S.

The tuning parameters for the D/S and S_f/S controllers are chosen as before: $\alpha_1 = 1\ h^{-1}$ and $\alpha_0 = 0.25\ h^{-2}$. The closed-loop performance of the D/S controller for the same test as in Fig. 8 is shown in Fig. 10. The controller attenuates oscillations in the controlled output S, but the damping is not as effective as that for the D/m_0 controller due to higher sensitivity to sampling. Moreover, the control moves are quite oscillatory and oscillations in the zeroth moment are barely attenuated. Although not shown here, similar results are obtained for the S_f/S controller. Consequently, these two controllers are less desirable than the D/m_0 controller despite the additional measurement required to implement the D/m_0 controller.

The different closed-loop responses generated by the three feedback linearizing controllers are difficult to predict *a priori*. Of particular interest are the differences observed in damping of the uncontrolled output. Below this behavior is analyzed for each controller using the closed-loop transfer function between the uncontrolled output and the setpoint. Linearization of the model Eqs. (10) at the steady-state operating point yields the transfer function matrix:

$$\begin{bmatrix} m_0(s) \\ S(s) \end{bmatrix} = \begin{bmatrix} g_{11}(s) & g_{12}(s) \\ g_{21}(s) & g_{22}(s) \end{bmatrix} \begin{bmatrix} D(s) \\ S_f(s) \end{bmatrix} \tag{17}$$

Denote the linearized controller transfer function for the D/m_0 pair as $g_c(s)$. The closed-loop system can be written as:

$$\begin{aligned} m_0(s) &= g_{11}(s) g_c(s) \left[m_0^*(s) - m_0(s) \right] \\ S(s) &= g_{21}(s) g_c(s) \left[m_0^*(s) - m_0(s) \right] \end{aligned} \tag{18}$$

The control objective is to make m_0 follow the second-order response defined by (13): $m_0(s) = g_d(s) m_0^*(s)$. The controller transfer function can be represented as:

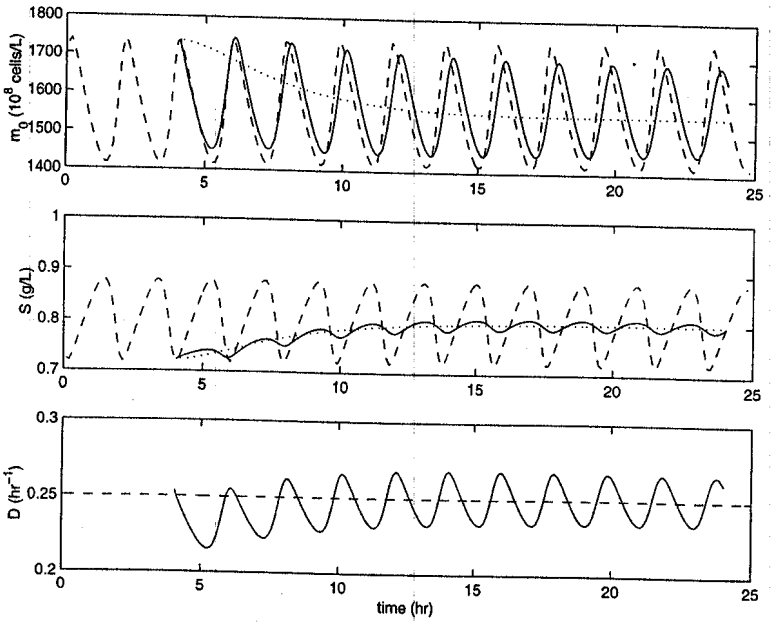

Fig. 10. Feedback linearizing control using the D/S pairing.

$$g_c(s) = \frac{1}{g_{11}(s)} \frac{g_d(s)}{1 - g_d(s)} \tag{19}$$

Therefore, the closed-loop response of the uncontrolled output S has the form:

$$S(s) = \frac{g_{21}(s)}{g_{11}(s)} g_d(s) m_0^*(s) \tag{20}$$

Similarly the closed-loop responses of the uncontrolled output m_0 for the D/S and S_f/S controllers are:

$$\begin{aligned} m_0(s) &= \frac{g_{11}(s)}{g_{21}(s)} g_d(s) S^*(s) \\ m_0(s) &= \frac{g_{12}(s)}{g_{22}(s)} g_d(s) S^*(s) \end{aligned} \tag{21}$$

respectively. Since $g_d(s)$ is chosen to have the form (13) and the open-loop transfer functions have the same poles, the zeros of the open-loop transfer functions $g_{ij}(s)$ are primarily responsible for the observed differences in the closed-loop response of the uncontrolled output variables.

Fig. 11 shows the zeros (z_i) of the transfer functions defined in (17). The transfer function g_{21} has several pairs of complex conjugate zeros very close to the imaginary axis, while the zeros of g_{11} are much further removed from the imaginary axis. This partially explains why oscillations in the substrate concentration are rapidly damped by the D/m_0 controller while the response of the zeroth moment is very oscillatory for the D/S controller. Similarly g_{22} has several pairs of complex conjugate zeros that are very close to the imaginary axis, which causes the m_0 oscillations to be slowly damped. Also note that g_{12} has a right-half-plane zero which would cause instability if the S_f/m_0 controller were designed and implemented.

Finally a MIMO feedback linearizing controller that regulates both m_0 and S by manipulation of D and S_f is designed. The design model (10) is rewritten below in state-space form where $x = [m_0 \ S \ S']^T$, $u = [D \ DS_f]^T$ and $y = [m_0 \ S]^T$:

$$\begin{aligned} \dot{x}_1 &= -x_1 u_1 + r(x_3) \\ \dot{x}_2 &= u_2 - x_2 u_1 - \frac{k(x_3)}{Y} m_0 \\ \dot{x}_3 &= \alpha(x_2 - x_3) \\ y &= \begin{bmatrix} 1 & 0 & 0 \\ 0 & 1 & 0 \end{bmatrix} x \end{aligned} \tag{22}$$

Here $r(x_3) \equiv \int_0^\infty \Gamma(m, S') W(m, t) \mathrm{d}m$ is the growth rate of the cell number concentration; it is assumed to be measured as before. Using standard input-output decoupling [13] the following control law is obtained:

$$\begin{bmatrix} u_1 \\ u_2 \end{bmatrix} = \begin{bmatrix} -\frac{1}{y_1} & 0 \\ -\frac{y_2}{y_1} & 1 \end{bmatrix} \left\{ v - \begin{bmatrix} r(x_3) \\ -k(x_3) y_1 \end{bmatrix} \right\} \tag{23}$$

where v is the two-dimensional input vector of the feedback linearized system. Each input v_i is designed as in (12):

$$v = -\begin{bmatrix} \alpha_1 & 0 \\ 0 & \beta_1 \end{bmatrix} y + \begin{bmatrix} \alpha_0 & 0 \\ 0 & \beta_0 \end{bmatrix} \int_0^t (y_{sp} - y) \mathrm{d}\tau \tag{24}$$

where α_i and β_i are tuning parameters.

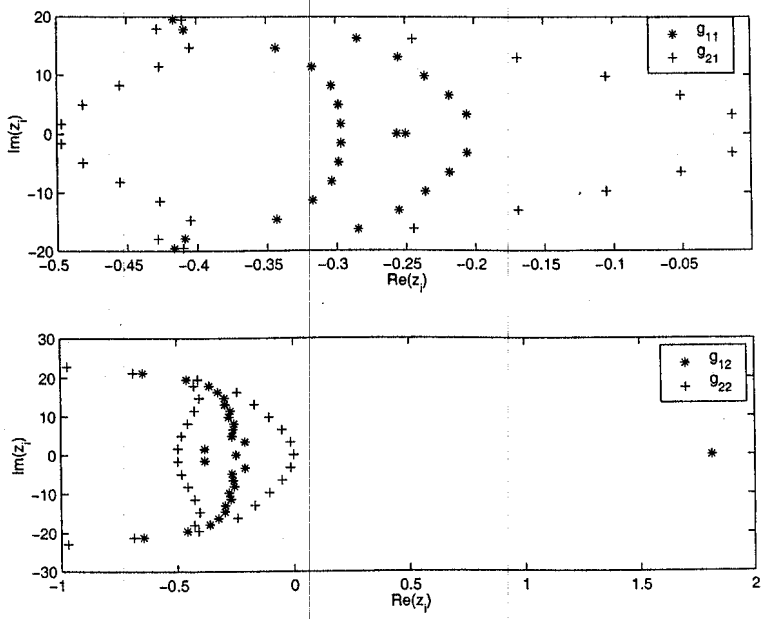

Fig. 11. Open-loop zeros of the moment model.

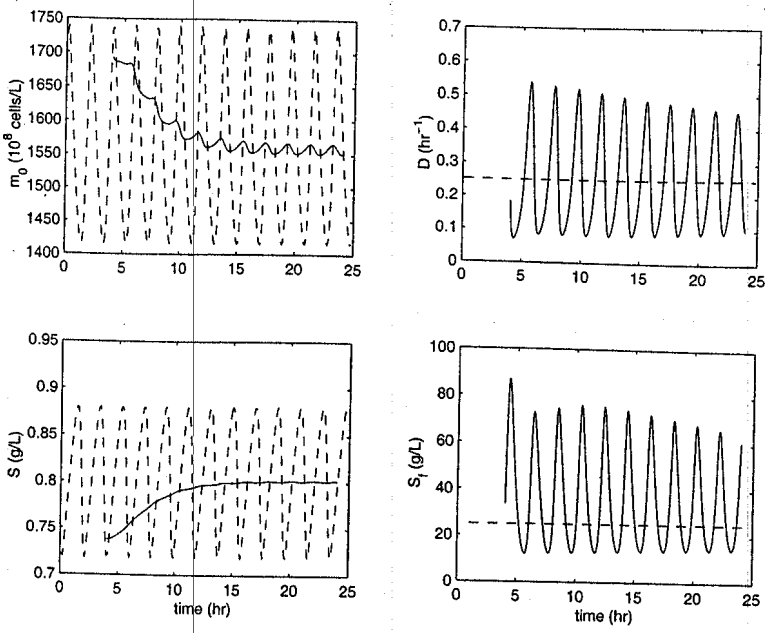

Fig. 12. MIMO feedback linearizing control.

The closed-loop response (—) of the MIMO controller is shown in Fig. 12. Also shown is the oscillatory response (- - - -) obtained in the absence of control. The tuning parameters used are $\alpha_1 = \beta_1 = 1\ \mathrm{h}^{-1}$ and $\alpha_0 = \beta_0 = 0.25\ \mathrm{h}^{-2}$. Both output variables are effectively regulated to their setpoints when the controller is turned on at $t = 4$ h. However, the control moves generated are excessive and preclude successful implementation of the controller on a real bioreactor. Therefore, the D/m_0 feedback linearizing controller appears to be the most promising option for oscillation attenuation.

5. Summary and conclusions

We have performed bifurcation analysis on a population balance equation (PBE) model for budding yeast cultures grown in continuous bioreactors. The model exhibits two supercritical Hopf bifurcations that are consistent with the spontaneous appearance and disappearance of sustained oscillations observed experimentally. However, there are some discrepancies between experimental data and the model simulation results. These include the speed of transition from sustained oscillations to steady state and the perplexing question of possible existence of multiple attractors under the same operating conditions. We hypothesize that the first problem can be attributed to the lack of chemical structure in the PBE model. The second problem needs to be investigated with additional experimental work. We have developed and evaluated four feedback linearizing controllers that employ different input-output variable pairings. Each controller is able to effectively attenuate oscillations in the controlled output variable(s), but the three SISO controllers have very different closed-loop responses for the uncontrolled output variable. The zeros of the linearized closed-loop system have been used to analyze this behavior.

Acknowledgements

Financial support from the National Science Foundation (Grant CTS-9501368) is gratefully acknowledged. The authors also would like to acknowledge Professors Yannis Kevrekidis and Jawahar Krishnan (Princeton) for supplying the continuation code and providing assistance with the bifurcation calculations.

References

[1] K.-H. Bellgardt, Analysis of synchronous growth of baker's yeast part I: development of a theoretical model for sustained oscillations, J. Biotechnol. 35 (1994) 19–33.

[2] M. Beuse, R. Bartling, A. Kopmann, H. Diekmann, M. Thoma, Effect of dilution rate on the mode of oscillation in continuous culture of *Saccharomyces cerevisiae*, J. Biotechnol. 61 (1998) 15–31.

[3] L. Cazzador, Analysis of oscillations in yeast continuous cultures by a new simplified model, Bull. Math. Biology 53 (1991) 685–700.

[4] L. Cazzador, L. Alberghina, E. Martegani, L. Mariani, Bioreactor control and modeling: A simulation program based on a structured population model of budding yeast, in: G.W. Moody, P.B. Baker (Eds.), Bioreactors and Biotransformations, Elsevier, London, 1987, pp. 64–75.

[5] G. Chen, Controlling Chaos and Bifurcations in Engineering Systems, CRC Press, New York, 2000.

[6] P. Duboc, U. von Stockar, Modeling of oscillating cultivations of *Saccharomyces cerevisiae*: Identification of population structure and expansion kinetics based on on-line measurements, Chem. Eng. Sci. 55 (2000) 149–160.

[7] A.G. Fredrickson, D. Ramkrishna, H.M. Tsuchiya, Statistics and dynamics of procaryotic cell populations, Math. Biosci. 1 (1967) 327–374.
[8] E. Heinzle, I.J. Dunn, K. Furukawa, R.D. Tanner, Modelling of sustained oscillations observed in continuous culture of *Saccharomyces cerevisiae*, in: Proc. IFAC Workshop on Modeling and Control of Biotechnological Processes, Helsinki, Finland, 1982, pp. 57–65.
[9] M.A. Hjortso, Periodic forcing of microbial cultures. A model for induction synchrony, Biotechnol. Bioengng. 30 (1987) 825–835.
[10] M.A. Hjortso, J.E. Bailey, Transient responses of budding yeast populations, Math. Biosci. 63 (1983) 121–148.
[11] M.A. Hjortso, J. Nielsen, A conceptual model of autonomous oscillations in microbial cultures, Chem. Eng. Sci. 49 (1994) 1083–1095.
[12] M.A. Hjortso, J. Nielsen, Population balance models of autonomous microbial oscillations, J. Biotechnol. 42 (1995) 255–269.
[13] A. Isidori, Nonlinear Control Systems, Springer, New York, 1989.
[14] K.D. Jones, D.S. Kompala, Cybernetic modeling of the growth dynamics of *Saccharomyces cerevisiae* in batch and continuous cultures, J. Biotechnolgy 71 (1999) 105–131.
[15] M.J. Kurtz, G.-Y. Zhu, A. Zamamiri, M.A. Henson, M.A. Hjortso, Control of oscillating microbial cultures described by population balance models, Ind. Eng. Chem. Res. 37 (1998) 4059–4070.
[16] Y.A. Kuznetsov, Elements of Applied Bifurcation Theory, Springer, New York, 1995.
[17] J.-J. Liou, F. Sirenc, A.G. Fredrickson, Solution of population balance models based on a successive generations approach, Chem. Eng. Sci. 52 (1997) 1529–1540.
[18] N.V. Mantzaris, J.-J. Liou, P. Daoutidis, F. Sirenc, Numerical solution of a mass structured cell population balance model in an environment of changing substrate concentration, J. Biotechnol., in press.
[19] E. Martegani, D. Porro, B.M. Ranzi, L. Alberghina, Involvement of a cell size control mechanism in the induction and maintenance of oscillations in continuous cultures of budding yeast, Biotechnol. Bioeng. 36 (1990) 453–459.
[20] P. Mhaskar, A.M. Zamamiri, M.A. Henson, M.A. Hjortso, A cell population model with structured medium for budding yeast cultures, in: Proc. Int. Conf. on Computer Applications in Biotechnology, Quebec City, Canada, in press.
[21] T. Munch, B. Sonnleitner, A. Fiechter, New insights into the synchronization mechanism with forced synchronous cultures of *Saccharomyces cerevisiae*, J. Biotechnol. 24 (1992) 299–313.
[22] S.J. Parulekar, G.B. Semones, M.J. Rolf, J.C. Lievense, H.C. Lim, Induction and elimination of oscillations in continuous cultures of *Saccharomyces Cerevisiae*, Biotechnol. Bioengng. 28 (1986) 700–710.
[23] D.E. Porro, B. Martegani, M. Ranzi, L. Alberghina, Oscillations in continuous cultures of budding yeasts: a segregated parameter analysis, Biotechnol. Bioeng. 32 (1988) 411–417.
[24] J.D. Sheppard, P.S. Dawson, Cell synchrony and periodic behavior in yeast populations, Canadian J. Chem. Eng. 77 (1999) 893–902.
[25] F. Srienc, Cytometric data as the basis for rigorous models of cell population dynamics, J. Biotechnol. 71 (1999) 233–238.
[26] F. Srienc, B.S. Dien. Kinetics of the cell cycle of *Saccharomyces cerevisiae*, in: Annuals of the New York Academy of Sciences, 1992, pp. 59–71.
[27] C. Strassle, B. Sonnleitner, A. Fiechter, A predictive model for the spontaneous synchronization of *Saccharomyces cerevisiae* grown in continuous culture. I. Concept, J. Biotechnol. 7 (1988) 299–318.
[28] C. Strassle, B. Sonnleitner, A. Fiechter, A predictive model for the spontaneous synchronization of *Saccharomyces cerevisiae* grown in continuous culture. II. Experimental verification, J. Biotechnol. 9 (1989) 191–208.
[29] G. Subramanian, D. Ramkrishna, On the solution of statistical models of cell populations, Math. Biosci. 10 (1971) 1–23.
[30] H.K. von Meyenburg, Stable synchrony oscillations in continuous culture of *Saccharomyces cerevisiae* under glucose limitation, in: B. Chance, E.K. Pye, A.K. Shosh, B. Hess (Eds.), Biological and Biochemical Oscillators, Academic Press, New York, 1973, pp. 411–417.
[31] A.M. Zamamiri, G. Birol, M.A. Hjortso, Multiple stable states and hysteresis in continuous, oscillating cultures of budding yeast, Biotechnol. Bioengng., submitted.
[32] Y. Zhang, G.-Y. Zhu, A.M. Zamamiri, M.A. Henson, M.A. Hjortso, Bifurcation analysis and control of yeast cultures in continuous bioreactors, in: Proceedings of the American Control Conference, Chicago, IL, 2000, pp. 1742–1746.
[33] G.-Y. Zhu, A.M. Zamamiri, M.A. Henson, M.A. Hjortso, Model predictive control of continuous yeast bioreactors using cell population models, Chem. Eng. Sci. 55 (2000) 6155–6167.